Article

Artificial Intelligence Prediction of Rutting and Fatigue Parameters in Modified Asphalt Binders

Ikenna D. Uwanuakwa [1,2,*], **Shaban Ismael Albrka Ali** [1], **Mohd Rosli Mohd Hasan** [2], **Pinar Akpinar** [1], **Ashiru Sani** [2,3] **and Khairul Anuar Shariff** [4]

[1] Department of Civil Engineering, Near East University, 99138 Nicosia, Mersin-10, Turkey; shabanismael.albrka@neu.edu.tr (S.I.A.A.); pinar.akpinar@neu.edu.tr (P.A.)
[2] School of Civil Engineering, Universiti Sains Malaysia, Engineering Campus, Nibong Tebal 14300, Penang, Malaysia; cerosli@usm.my (M.R.M.H.); ashiru@student.usm.my (A.S.)
[3] Department of Civil Engineering, Kano University of Science and Technology, 3011 Wudil, Kano, Nigeria
[4] School of Material and Mineral Resources Engineering, Universiti Sains Malaysia, Engineering Campus, Nibong Tebal 14300, Penang, Malaysia; biokhairul@usm.my
* Correspondence: ikenna.uwanuakwa@neu.edu.tr

Abstract: The complex shear modulus (G*) and phase angle (δ) are fundamental viscoelastic rheological properties used in the estimation of rutting and fatigue pavement distress in asphalt binder. In the tropical regions, rutting and fatigue cracking are major pavement distress affecting the serviceability of road infrastructure. Laboratory testing of the complex shear modulus and phase angle requires expensive and advanced equipment that is not obtainable in major laboratories within the developing countries of the region, giving rise to the need for an accurate predictive model to support quality pavement design. This research aims at developing a predictive model for the estimation of rutting and fatigue susceptive of asphalt binder at intermediate and high pavement temperatures. Asphalt rheological and ageing test was conducted on eight mixes of modified binders used to build the study database containing 1976 and 1668 data points for rutting and fatigue parameters respectively. The database was divided into training and simulation dataset. The Gaussian process regression (GPR) algorithm was used to predict the rutting and fatigue parameters using unaged and aged conditioned inputs. The proposed GPR was compared with the support vector machine (SVM), recurrent neural networks (RNN) and artificial neural network (ANN) models. Results show that the model performed better in the estimation of rutting parameter than the fatigue parameter. Further, unaged input variables show better reliability in the prediction of fatigue parameter.

Keywords: GPR; SVM; rutting; fatigue; machine learning; modified binder

1. Introduction

In asphalt pavement construction, the selection of appropriate asphalt binder with the required properties to mitigate the challenges of pavement deterioration is critical in prolonging the service life of the asphalt pavement exposed to ageing conditions. Asphalt binder, within the asphalt, dominates the viscoelastic properties of the asphalt pavement subjected to various pavement distresses. Rutting and fatigue cracking are serious pavement distresses facing asphalt pavement that are exposed to intermediate and high temperatures prevailing in the tropical regions [1–5]. Rutting in asphalt pavement occurs as a result of accumulated strain which induces a non-recoverable deformation along the wheel path of the pavement [6]. The plastic deformation that is formed along the wheel path creates discomfort to the road user and reduces the service life of the pavement. On the other hand, fatigue cracking develops in asphalt pavement due to repeated loading on the asphalt pavement

surface. Fatigue cracking is caused by weak, sub-grade, base and poor material design, and reduced strain tolerance of the asphalt mixture resulting from long-term field ageing [1,7]. The selection of appropriate asphalt binder has been reported to enhance the resistance of hot mix asphalt (HMA) concrete when subjected to rutting and fatigue [2,8,9]. Further, laboratory testing of rutting and fatigue in asphalt binder requires advanced testing equipment that is not readily available in the developing countries within the tropical regions. However, governments are saddle with the responsibility of providing quality pavement structure with the limited available budget. In such cases, the application of a predictive model would reduce project cost and deliver quality pavement structure.

The existing predictive models studies in pavement construction mainly focused on predicting the concrete dynamic modulus (E*), complex shear modulus (G*) and phase angle of the binder. These models do not account for the binder selection for rutting and fatigue cracking resistance in a pavement structure [10–12], which this study seeks to address using machine learning models.

Machine learning within the last few years has made its presence felt in various sectors; on the internet [13], communication system [14,15], vision and voice recognition [16–19], smart device and instrumentations [20], as well as other engineering applications [21–24]. Its deployment has witnessed unprecedented results and revolution in the filed of artificial intelligence. Computational methods available in machine learning field include the artificial neural networks, support vector machine, Gaussian process regression, recurrent neural networks and others. The artificial neural networks (ANN) is an artificial intelligence-based algorithm that uses the abstraction of the biological neural networks. Although ANN performance in literature has been reported to have good predictive results, it is often criticised for having high computational cost (iteration tuning) and for often trapped at a local minimum. Further, data overfitting is another disadvantage critics observed about ANN; that is, the inability of the model to correctly map new inputs to corresponding target values [25,26]. To overcome these problems, a non-parametric approach such as Gaussian process minimises the data overfitting by defining a distribution function and setting an initial distribution to unlimited possibilities over the function directly [27]. Comparative studies of Gaussian process regression (GPR) and other machine learning tools such as ANN and support vector machine (SVM) show that the algorithm is an efficient machine learning tool with higher accuracy on the generalisation data set [27–33].

In the asphalt technology field, machine learning models have been widely reported to have higher predictive accuracy over regression models [34–38]. The traditional artificial neural networks, support vector machine and decision tree algorithm have been applied in different study areas with higher predictive accuracy over regression models.

A number of literatures exist on the application of machine learning modeling in asphalt binder and hot mixed asphalt (HMA) concrete, Ghasemi et al. [34], predicted hot mixed asphalt (HMA) concrete dynamic modulus using the ANN and multivariable regression models. The study's selected input variables were drawn from features of volumetric and particles size gradation of nine mixes to extract 243 data points. Further, principal component analysis was used for orthogonal transformation and resulting principal components were used to calibrate the ANN and multivariable regression models. The results of the fitted test data show that the ANN model satisfactorily estimated the dynamic modulus (E*) of the HMA. Daneshvar and Behnood, [39], on the other hand, compared the performance random forest algorithm with Witczak model in the prediction of E* of HMA. Using the statistical parameters (R^2 and average errors), the study concluded that the developed model improved the E* as compared to Witczak models. El-Badawy et al. [40], compared the traditional ANN and three existing regression models (Witczak NCHRP 1-37A, Witczak NCHRP 1-40D and Hirsch) in the prediction of E* in HMA concrete using 25 mixes each, from the Kingdom of Saudi Arabia and Idaho State. A total of 3720 cases were extracted from the 50 mixes to build the research database. Three ANN models were evaluated using input variables from the three-existing regression models. The research concluded that Witczak models are more effective in the prediction of E* when compared to the Hirsch model. Further, the input parameters in Witczak NCHRP 1-37A were reported to show

a more dynamic effect on the sensitivity scale when compared with Witczak NCHRP 1-40D model inputs variables that were dominated by binder properties. The three evaluated ANN models proved to have improved E* value when compared with the corresponding regression models. A similar research to El-Badawy et al. [40], was conducted by Liu et al. [36]) with the incorporation of recycled asphalt shingles (RAS) and comparison of ANN model and modified Witczak E* model developed by Yu [41]. The developed ANN model also showed improved E* values when compared to Yu RAS model. Further, few studies [10–12,42] on machine learning prediction of complex modulus and phase angle did not account for ageing conditioning in asphalt binder. This limited their findings in the prediction of rutting and fatigue parameters in the asphalt binder.

Existing literature accounted for a predictive model for dynamic modulus (E*) in asphalt mixture. For example, the Witczak model can predict E* using parameters that can be extracted from a basic experiment and manufacturer's specifications. The model is cost effective in mechanistic-empirical pavement design guide (MEPDG). However, predictive models for the design of mixture parameters cannot standalone without a complimentary binder model [43].

The objective of this study is to develop an efficient predictive model for the selection of binder to resist rutting and fatigue cracking in the asphalt pavement structure at intermediate and high temperatures by the inclusion of a novel approach of employing unaged parameters together with GPR algorithm for the prediction of rutting and fatigue cracking. The sections below explain, in detail, the methodology employed for this objective and the results indicating the obtained success in the prediction of rutting and fatigue cracking in asphalt pavements.

2. Materials and Methods

In this study, 8 mixes of Styrene-butadiene-styrene) (SBS) polymer and latex modified asphalt binder were used to build the database. The SBS used were Kraton® D1152 ESM and D1101 ASM linear polymers, while the latex was natural rubber from Penang region of Malaysia. The SBS were added at 3, 5 and 7% by weight of the control asphalt binder, while the latex was added by 3 and 6% by weight of the control asphalt binder.

The main objective of this research is to evaluate an alternative model that can be used in the selection of asphalt binder for a particular PG (performance grade) temperature from the results of the basic rheological test. A frequency sweep test using the dynamic shear rheometer (DSR) equipment was used to measure the phase angle (δ) and complex shear modulus (G*) at different test temperatures.

Assessment of G/sinδ rutting parameter*: The variation of the parameter was investigated on rolling thin film oven (RTFO) conditioned binder at temperatures between 46 °C to 76 °C, at 6 °C increments. The test was carried out according to the procedures specified in AASHTO T 315. The rutting resistance of asphalt binder is measured by G*/sinδ.

Assessment of G.sinδ fatigue property*: The residue of the rolling thin film oven (RTFO) test conditioned binder was used in the long-term aged binder conditioning using the pressure-ageing vessel (PAV) test. The DSR test was performed on an 8 mm parallel plate with 2 mm gap to measure the parameters for fatigue property evaluation. The test was carried out in accordance with AASHTO T 315 standard specification between 16 to 31 °C at 3 °C increments. The fatigue resistance of asphalt binder is measured by G*.sinδ.

2.1. Case Studies

Three case studies were investigated. The first case study involves the prediction of the rutting parameter (G*/sinδ) using the unaged parameter from the DSR test, viscosity and softening point test. In the second case study, the prediction of the fatigue parameter (G*.sinδ) with the unaged input variables was proposed. Finally, the third case study involved replacing the unaged DRS variables in the second case study with the RTFO test variables.

2.2. Data Preparation and Model Architecture

The results of the material characterisation and mechanical dynamic test were used to build the database for the machine learning modelling. The input variables consist of 16 variables; softening point (°C), viscosity (Pa.s) at 135 °C, DSR test frequency (rad), temperature (°C), phase angle (°) and complex shear modulus (kPa) at test temperatures between 46–76 °C at 6 °C increment. The databases consist of 1980 and 1668 data points for the modelling rutting and fatigue parameters respectively. The database was divided into training and simualtion sets. The training set was further divided into training-testing-validation subsets. The details of the mix and the corresponding data point are presented in Table 1. The output for the first case study (1) was the Superpave® rutting parameter (G*/sinδ), and for the second (2) and third (3) case studies was the Superpave® fatigue parameter (G*.sinδ). The descriptive statistic of the data used is presented in Table 2. After data collection, the binary normalisation was applied to both the input and output variables independently. While the normalisation is important to reduce early saturation during training, it can also reduce the importance of certain variables with smaller numeric values. In order to avoid scaling down of any variables, the normalisation was applied within the variables [44,45].

Table 1. Research mix design.

Mix Code	Modifier	% Added	Density g/cm^3	Data Point Case Study		
				1	**2**	**3**
M-SB-3A	SBS D1152	3	0.40	312	260	260
M-SB-3B	SBS D1101	3	0.40	156	130	130
M-SB-5A	SBS D1152	5	0.40	464	390	390
M-SB-5B	SBS D1101	5	0.40	312	260	260
M-SB-7A	SBS D1152	7	0.40	312	260	260
M-SBS 1	SBS D1101	7	0.40	312	260	260
M-L-3	Latex	3	0.92	54	54	54
M-L-6	Latex	6	0.92	54	54	54

Table 2. Statistical description of the measured 18 input variables and the outputs.

Variables	Modelling of Rutting with Unaged Binder Inputs				Modelling of Fatigue with Unaged Binder Inputs				Modelling of Fatigue with RTFOT Binder Inputs			
	Min	Max	Mean	Std. Deviation	Min	Max	Mean	Std. Deviation	Min	Max	Mean	Std. Deviation
Frequency (rad)	0.63	62.80	15.06	18.44	0.63	62.80	15.06	18.44	0.63	62.80	15.06	18.44
Softening point (°C)	50.00	70.25	57.63	6.82	50.00	70.00	57.63	6.82	54.00	79.00	62.17	8.16
Viscosity (Pas)	1131.50	3204.30	1926.99	689.74	1132.00	3204.00	1926.99	689.78	1131.50	3204.30	1926.99	689.78
G* @ T46 °C (kPa)	5070.00	294,000.00	78,123.08	72,387.62	5070.00	294,000.00	78,123.08	72,391.49	12,000.00	637,000.00	145,668.60	135,273.40
G* @ T52 °C (kPa)	1990.00	149,000.00	38,442.69	36,095.25	1990.00	149,000.00	38,442.69	36,097.18	4500.00	290,000.00	70,249.23	64,701.79
G* @ T58 °C (kPa)	775.00	79,700.00	18,902.45	18,644.12	775.00	79,700.00	18,902.45	18,645.12	1620.00	152,000.00	32,862.05	31,843.26
G* @ T64 °C (kPa)	333.00	48,400.00	10,366.33	10,690.06	333.00	48,400.00	10,366.33	10,690.63	690.00	75,600.00	18,163.12	17,692.36
G* @ T70 °C (kPa)	153.00	28,300.00	5606.22	5897.43	153.00	28,300.00	5606.22	5897.74	312.00	47,800.00	9935.94	9943.40
G* @ T76 °C (kPa)	78.50	16,500.00	3351.97	3465.50	79.00	16,500.00	3351.97	3465.69	156.00	27,000.00	6029.82	5871.54
δ @ T46 °C (°)	40.10	88.90	63.10	9.07	40.00	89.00	63.10	9.07	37.20	88.40	58.48	8.38
δ @ T52 °C (°)	48.50	85.30	66.63	8.12	49.00	85.00	66.63	8.13	39.00	77.40	62.14	7.82
δ @ T58 °C (°)	51.40	88.20	69.54	8.54	51.00	88.00	69.54	8.54	49.00	81.90	65.52	7.18
δ @ T64 °C (°)	48.00	89.80	71.68	9.55	48.00	90.00	71.68	9.55	48.60	85.60	68.41	8.52
δ @ T70 °C (°)	28.40	89.60	72.02	12.74	28.00	90.00	72.02	12.74	22.80	89.60	69.34	11.85
δ @ T76 °C (°)	22.80	89.90	72.15	14.77	23.00	90.00	72.15	14.77	14.30	89.90	69.17	15.95
Temperature °C	46.00	76.10	61.00	10.25	16.00	31.00	23.20	5.57	16.00	31.20	23.20	5.56
Output (kPa)	0.16	796.56	55.34	95.48	30,328.00	1,555,500.00	361,493.90	277,693.70	30,327.70	1,555,500.00	361,493.90	277,693.70

2.3. Research Model

Three models consisting of the Gaussian process regression (GPR), artificial neural networks (ANN) and recurrent neural networks (RNN) using the MATLAB software for all the algorithm.

The research model architecture is presented in Figure 1. In the model development, the model was trained with the combined six SBS mixes, while the remaining latex mixes were reserved for simulation of the developed model. The idea is to assess the performance of the model with an independent test replica dataset that was not used to calibrate the model. The independent dataset provides a measure of the accuracy of a trained model.
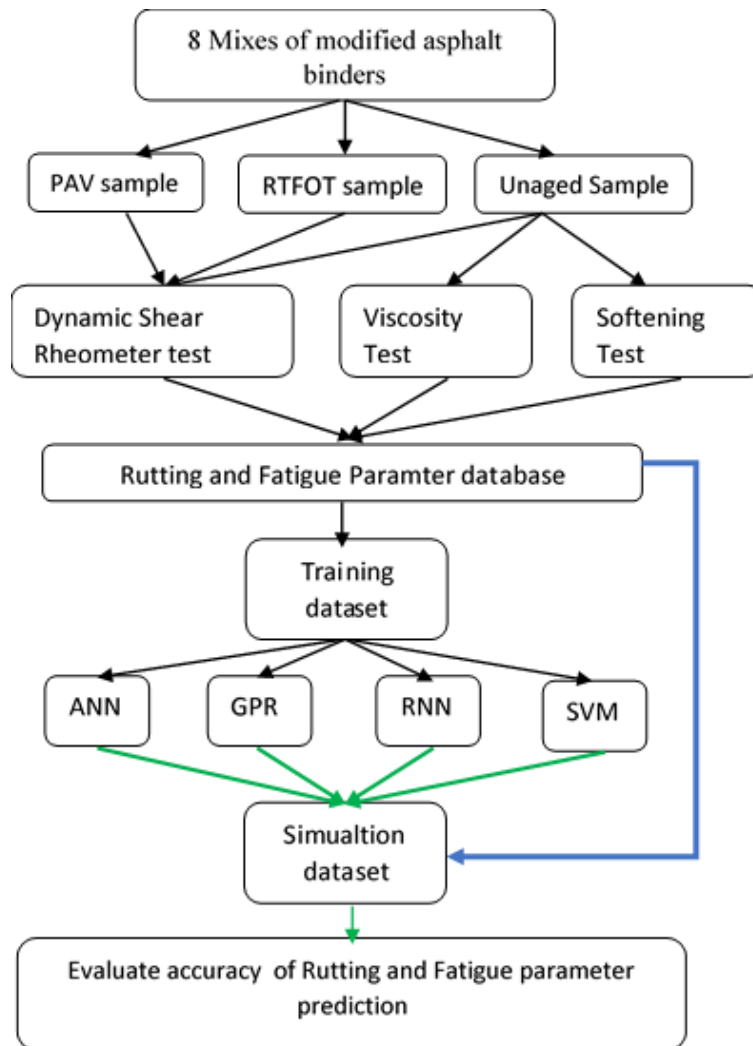
Figure 1. Model Architecture.

The developed model performance was measured using a cost function that penalises or reward the network. The network mean-square-error (MSE) was the cost function used in this research. Further, the ANN and RNN samples were divided into mini-batches in a ratio of 60:20:20 and 70:15:15 training:testing: validation sets respectively. A five-fold cross-validation was applied to the GPR models and trained using the regression learner App in the MATLAB software. The network parameters were obtained and updated through trial and error. A total of 12 hidden neurons were found to be sufficient for ANN and RNN models. The GPR kernel function was set to square exponential. The computations were carried out on Intel Corei3, 2.10 GHz CPU on Windows 10 with 12 GB RAM.

2.4. Model Evaluation Criteria

In machine learning modelling, different evaluation criteria are used to quantify the performance of the model. According to Wu and Chau (2013), evaluation of model performances should include absolute and relative error measurements of the model [46]. In this study, two traditional statistical tools were used: the coefficient of determination (R^2); the root mean squared error (*RMSE*) and the mean absolute error (*MAE*).

$$R^2 = \frac{SSR}{SST} \tag{1}$$

$$RMSE = \sqrt{\frac{\sum_{i=1}^{N}(Y_{Predi} - Y_{Obi})^2}{n}} \tag{2}$$

$$MAE = \frac{1}{n}\sum_{i=1}^{N}|Y_{Obi} - Y_{Predi}| \tag{3}$$

where n is the number of observed values, Y_{Pred1}. Y_{Pred2}. ...... Y_{PredN} are predicted values; Y_{Ob1}. Y_{Ob2}. ...... Y_{ObN}. are the observed values; SSR is the sum of squared regression derived by $\sum \left(Y_{Predi} - \overline{Y}\right)^2$; SST is the total variation contained in the dataset derived by $\sum \left(Y_{Obi} - \overline{Y}\right)^2$ and $\overline{Y}$ is the mean of Y value.

3. Results and Discussion

3.1. Prediction of Rutting Parameter (G*/sinδ) Using Unaged Parameters

The results of the prediction of the Superpave® rutting parameter are presented in Table 3 and Figure 2. The main motivation of this section is to explore the possibilities of using an unaged input parameter to predict the Superpave® (G*/sinδ) rutting parameter. As stated in the previous section, the G*/sinδ parameter is valuable in estimating rutting susceptive in asphalt binder. However, experimental measurements to determine the values of G*/sinδ at different PG (performance grade) temperatures is expensive and involve advanced equipment.

Table 3. Performance results for the prediction of G*/sinδ parameters using unaged dataset.

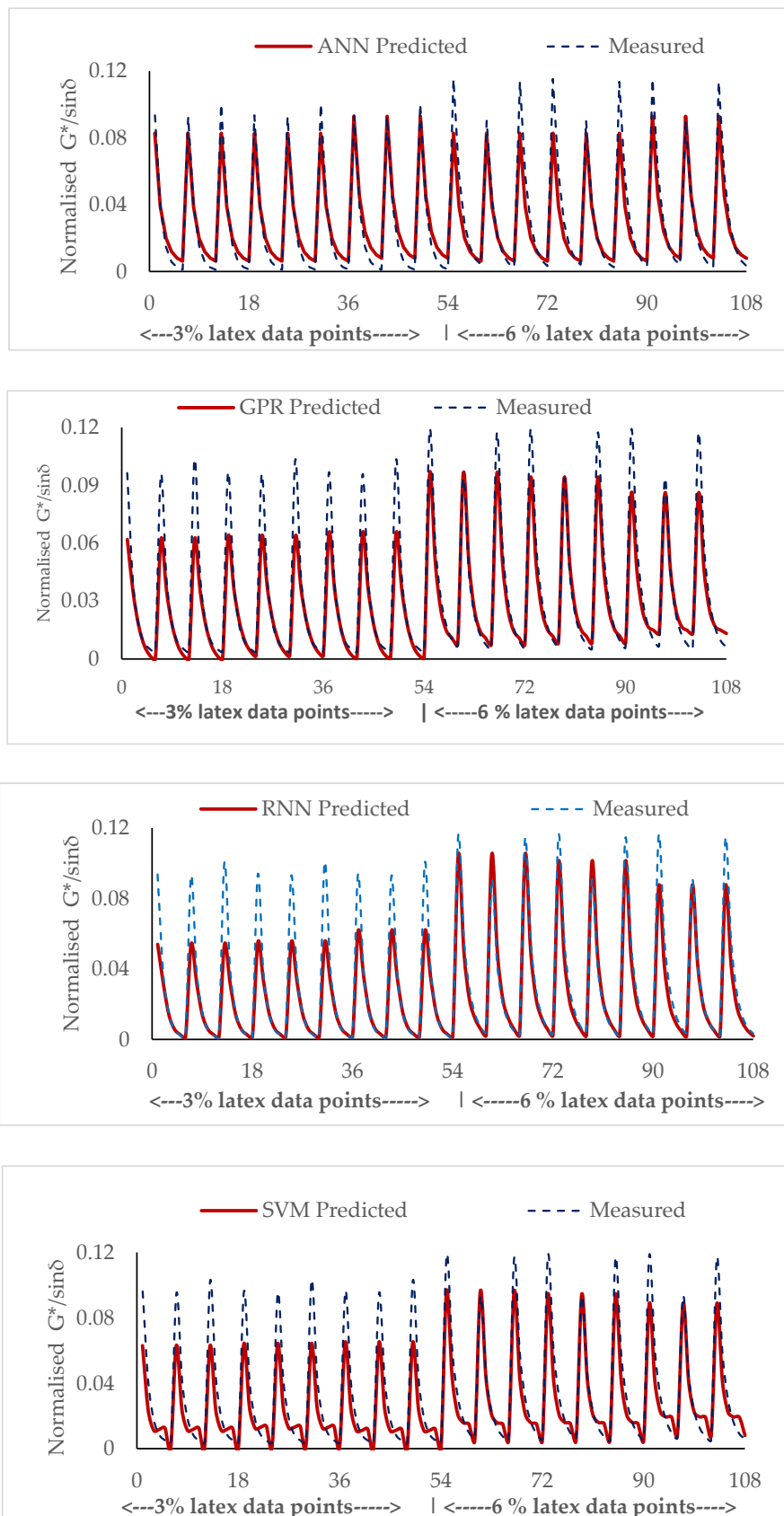| Model	Training Results			Simulation Results					
				3% Latex Dataset			6% Latex Dataset		
	R^2	RMSE	MAE	R^2	RMSE	MAE	R^2	RMSE	MAE
ANN	0.96	0.024	0.013	**0.99**	**0.007**	**0.006**	0.96	0.012	0.008
GPR	0.95	0.026	0.012	0.97	0.015	0.008	0.97	0.010	0.007
RNN	0.97	0.019	0.010	0.96	0.016	0.008	**0.96**	**0.008**	**0.005**
SVM	0.95	0.028	0.013	0.95	0.016	0.012	0.95	0.011	0.008

Figure 2. The comparison of predicted vs. measured G*/sinδ parameters using the unaged dataset.

Four different approaches were used for modelling of the G*/sinδ parameter at different PG temperatures. The proposed GPR algorithm, RNN, SVM and the ANN were the modelling tools used.

In the results, it is worth noting that the overall training performance of the four methods was satisfactory considering the normalized RMSE, MSE and MAE values and coefficient of determination (R^2) of the models. The statistical goodness of fit parameters is presented in Table 3. A comparison could be made between the GPR and RNN predictive accuracy and traditional ANN and SVM models. Figure 2 shows the point by point comparison of the combined (M-L-3 and M-L-6) simulation dataset results of the unaged dataset prediction of rutting parameter. As seen from the graph, the ANN model was able to simulate the corresponding measured rutting parameters better than the GPR, RNN and SVM with respect to R^2 values of 0.99 and 0.96 for the M-L-3 and M-L-6 simulation subsets respectively. The normalised RMSE and MAE were also found to be lower than the other models, The overall performance of all the models was substantially high.

3.2. Prediction of Fatigue Parameter (G*.sinδ) Using Unaged Parameters

A major objective of evaluating the methods for predicting fatigue resistance in asphalt binder is to eliminate the laborious laboratory works involved in measuring fatigue performance in the binder. The modelling of fatigue resistance of the asphalt binder is critical in prolonging the service life of the pavement. The evaluation of binder fatigue resistance requires short and long term aged conditioning resulting in physical and chemical changes in the binder.

The performance of the models is presented in Table 4 and a graphical representation of the point by point comparison of the predicted and measured values for the simulation dataset is in Figure 3.

Table 4. Performance results for the prediction of fatigue parameter (G*.sinδ) parameters using unaged dataset.

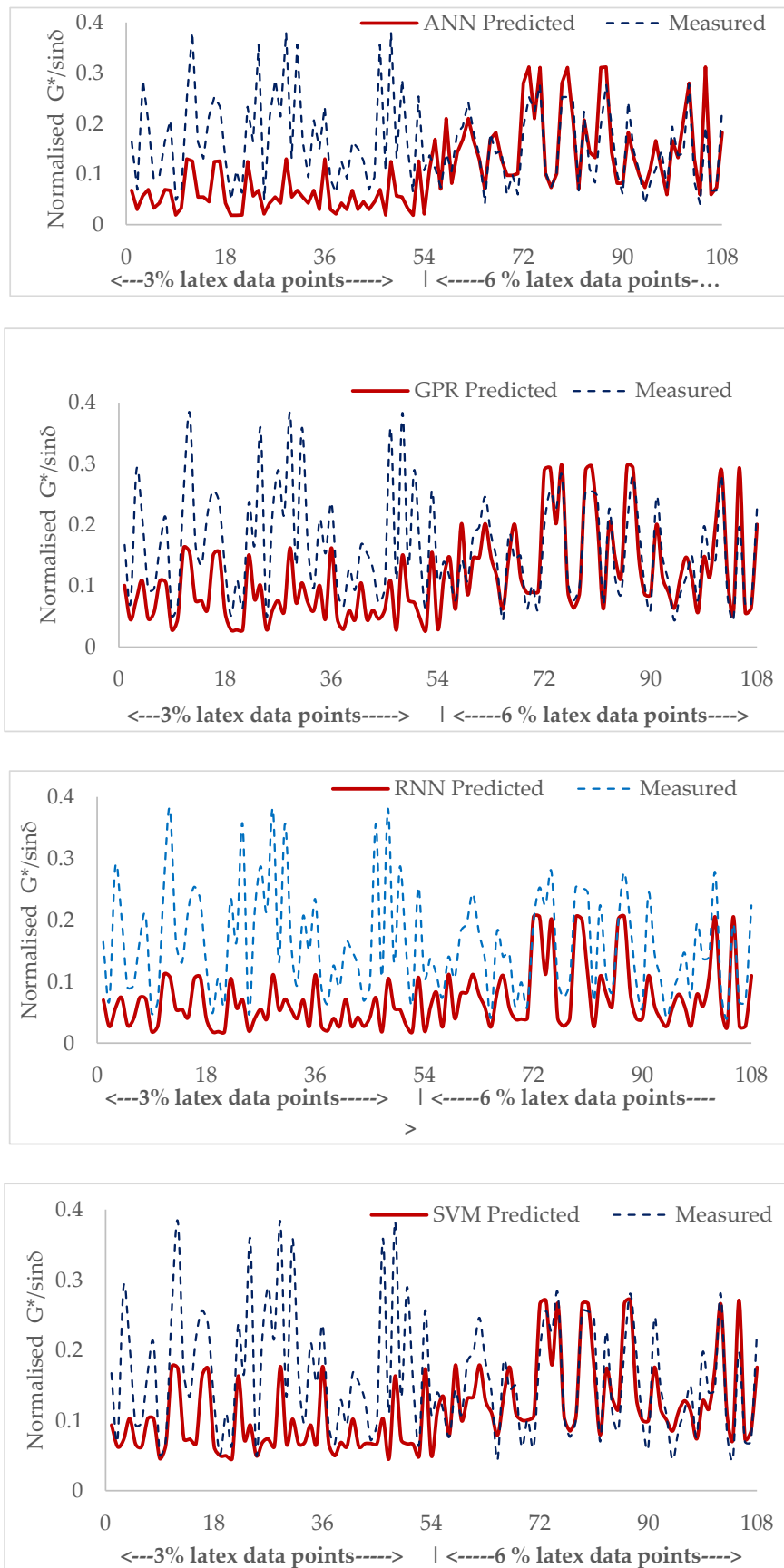| Model	Training Results			Simulation Results					
				3% Latex Dataset			6% Latex Dataset		
	R^2	RMSE	MAE	R^2	RMSE	MAE	R^2	RMSE	MAE
ANN	0.98	0.028	0.020	0.49	0.116	0.090	0.70	0.039	0.032
GPR	0.96	0.036	0.024	**0.60**	**0.120**	**0.019**	**0.76**	**0.38**	**0.032**
RNN	0.98	0.028	0.020	0.61	0.142	0.121	0.70	0.071	0.061
SVM	0.96	0.037	0.025	0.49	0.116	0.090	0.70	0.039	0.032

Figure 3. The comparison of predicted vs. measured G*.sinδ parameters using the unaged dataset.

The results in Table 4 show that all model training performed substantially well. However, high model training accuracy does not translate to performance with a simulation of a new dataset that was not previously used in the model calibration. All the models did not perform well with M-L-3 mix simulation dataset. However, the proposed GPR within the two mixes (M-L-3 and M-L-6) used for simulation performed better than ANN, RNN and SVM models. The poor performance of the models at 3% latex modification could be attributed complex chemical and physical changes that takes place during short and long term binder ageing conditioning.

With 76% correlation between the predicted and the measured value of G*.sinδ parameter using the GPR model, it is possible to eliminate the ageing conditions (PAV and RTFOT) test required in the selection of suitable binder that meets specified PG temperature criteria for medium and low density traffic. This could be beneficial to the developing countries within the tropical region who need to use the manufacture specification data to design pavement structures.

3.3. Prediction of Fatigue Parameter (G*.sinδ) Using Short-Term Aged Parameters

Further, in the previous section, the essence of using the unaged input variables is to reduce the prediction cost for the prediction of the fatigue parameter. However, in this case study, the RTFO conditioned dataset was used to evaluate the progress of G*.sinδ parameter in the asphalt binder. Although the modelling cost is higher, this research aimed to investigate the reliability of modelling G*.sinδ parameter using the GPR algorithm.

The results of the four algorithms show higher training accuracy for the modelling of G*.sinδ parameter using the short-term aged input variables as shown in Table 5 and Figure 4. As observed in Section 3.2, the simulation performance were lower than the training performance. The poor performance of the models especially, with 3% latex modification imply that the training dataset is insufficient for extracting the complex chemical and physical changes features that take place during binder ageing. The complexity of binder ageing can be seen in the bahaviours of the model with 3% latex modification.

Table 5. Performance results for the prediction of fatigue parameter (G*.sinδ) parameters using short-term aged dataset.

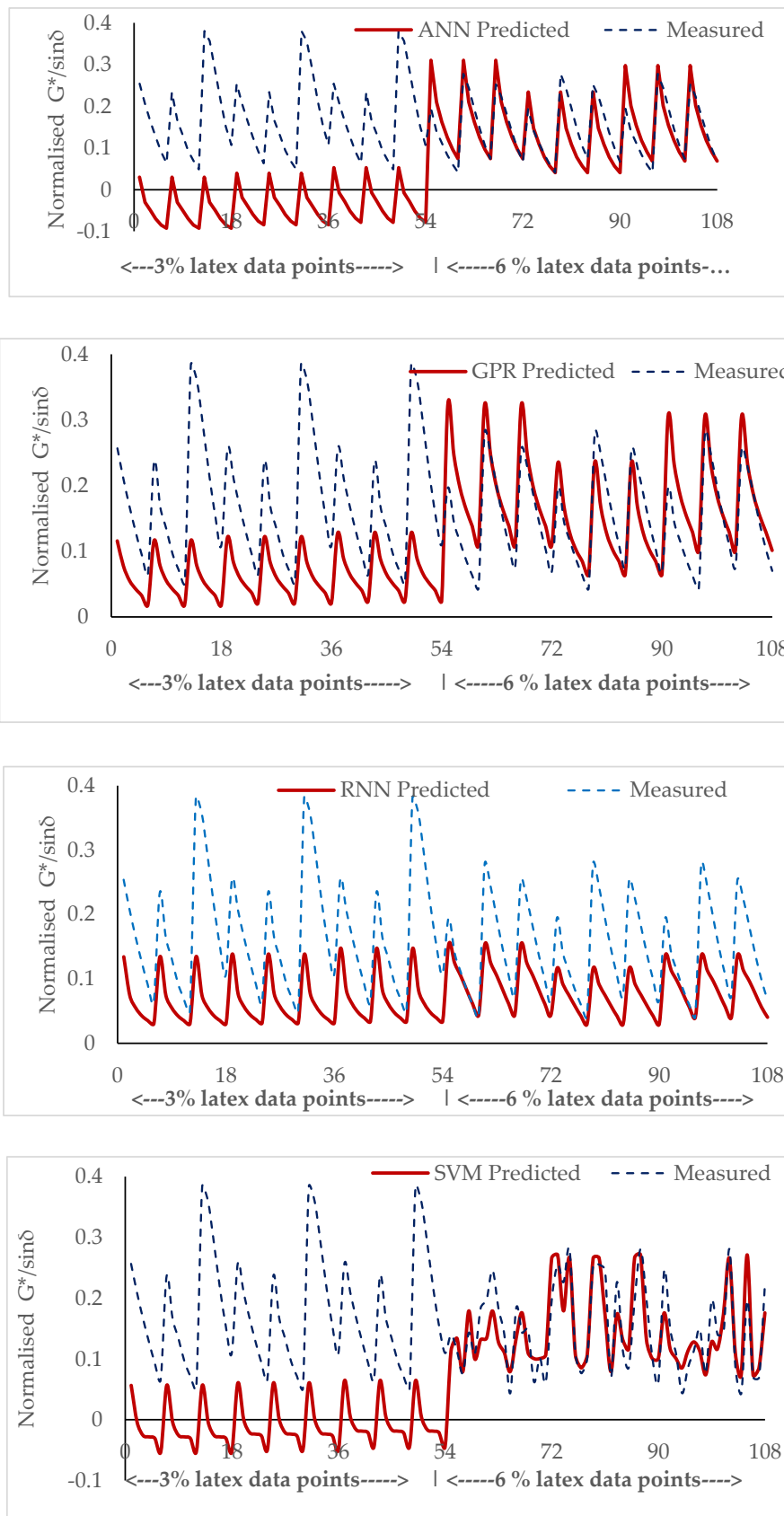| Model	Training Results			Simulation Results					
				3% Latex Dataset			6% Latex Dataset		
	R^2	RMSE	MAE	R^2	RMSE	MAE	R_2	RMSE	MAE
ANN	0.98	0.027	0.019	0.50	0.225	0.214	**0.68**	**0.044**	**0.035**
GPR	0.96	0.036	0.025	**0.60**	**0.136**	**0.116**	0.64	0.050	0.040
RNN	0.97	0.029	0.021	0.52	0.132	0.110	0.71	0.077	0.063
SVM	0.96	0.035	0.025	0.50	0.201	0.187	0.66	0.045	0.036

Figure 4. The comparison of predicted vs. measured G*.sinδ parameters using the short-term aged dataset.

3.4. Parameter Sensitivity Analysis

Computational models have, in recent time, paved the way for providing optimal solution to a design problem. Its reliability is dependent on the features of the selected model parameters that add uncertainty to the model output. However, model parameter uncertainty on the output can be evaluated using a structural optimisation design method called the sensitivity analysis (SA). Global sensitivity analysis (GSA) is a class of SA that provides valuable global insight on how the model output variance is dependent on the uncertainty of a particular model parameter by allowing more than one factor to vary at the same time [47,48].

In this study, the GSA was applied using the easy GSA MATLAB solution. The study by Al et al. (2019) contains a detailed development with research data for easy GSA. The Sobol first and total order indices were used to estimate model parameter sensitivity to output variance. The Sobol index is a sensitivity index that decomposes the output variance and estimate the importance of a single or specific set of variables in the uncertainty of the model output [47]. The first order accounts for individual effects on the variance of the dependent variable. On the other hand, the total indices account for the overall dependent variable effect on the model output variance and also inter-variable interactions [48].

3.4.1. Sensitivity Analysis of Rutting Model Parameters

With respect to the unaged parameters on the G*/sinδ, which was the scope of the Case Study-1, Figure 5 shows that the temperature, softening point and test frequency are the most influencing parameters. Further, the influence of phase angle showed a unique trend with the phase angle at T58 °C recording the highest STi value. The results are in agreement with the standard laboratory values; increase in test temperature and frequency decrease the G*/sinδ values of asphalt binder. Further, the importance of viscous and elastic properties of asphalt binder that influences the rutting behaviour observed in the phase angle and softening point values.
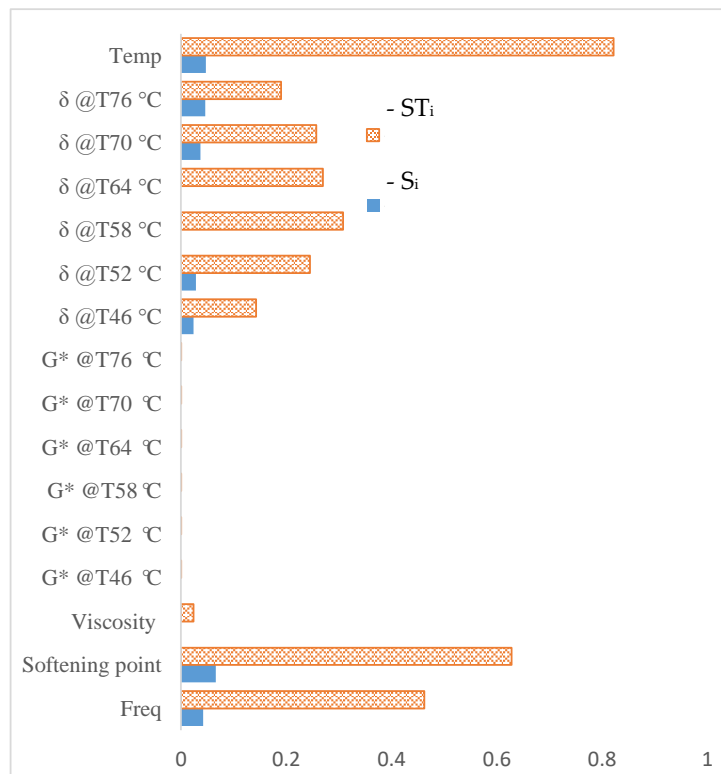

Figure 5. Sobol indices obtained for rutting model parameters.

3.4.2. Sensitivity Analysis of Fatigue Model Parameters

The objectives of Case Studies 2 and 3 were to predict the fatigue cracking using unaged and short-aged (RTFOT) parameters respectively. This study only focused on the prevailing temperature range affecting tropical regions. As obtained in Case Study 1, the phase angle, softening point and test temperature and frequency showed high sensitivity to the variation of $G^*.\sin\delta$ parameter. The Sobol indices showed low sensitivity of G^* and viscosity of the binder to the variation of $G^*.\sin\delta$ parameter as shown in Figure 6.
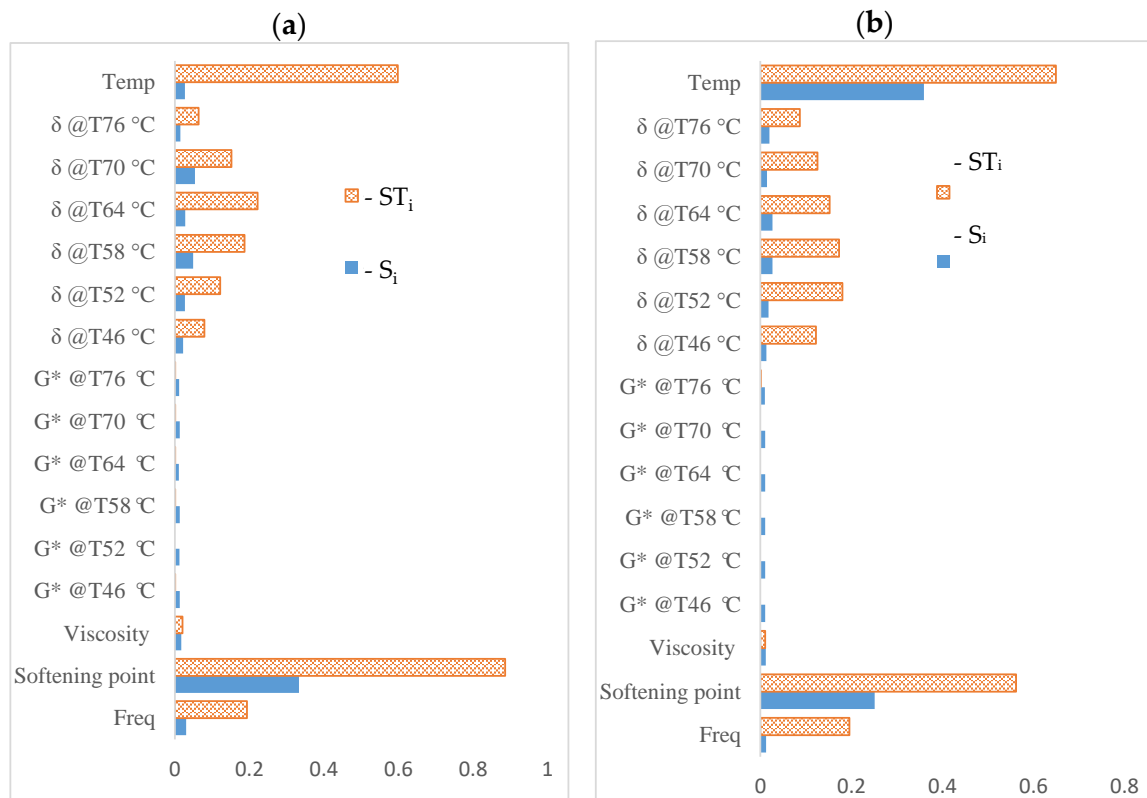

Figure 6. Sobol indices obtained for fatigue model using (**a**) unaged parameters and (**b**) RTFOT parameters.

4. Conclusions

In this study, the reliability of the GPR algorithm was evaluated for the prediction of rutting and fatigue cracking in the binder. For this aim, six SBS and two latex modified binders were used to build the study database. The SBS modified binders were used to train the model, while latex modified binders were reserved for simulation of the models. Three case studies were evaluated using unaged and short-term aged input variables to predict rutting and fatigue parameters. The motivation was to provide a predictive model to support pavement designers in tropical regions with limited highway laboratory equipment. The designers may rely on manufacturer's specifications and basic binder test to evaluate the performance of the selected binder at intermediate and high temperatures. The performance of the GPR model was verified against the traditional ANN, SVM and RNN models. The proposed GPR model showed comparable performance with ANN, SVM and RNN models. Thus, the study draws the following conclusions:

1. Prediction of rutting parameter with unaged variables yielded a significant higher accuracy of 97% correlation with measure values with the GPR model on the simulation dataset.

2. The selected input variables and database was not sufficient to predict fatigue parameters at intermediate temperature. This resulted to underestimation of the fatigue parameter in Case Studies 2 and 3.

3. The results further indicated that the unaged input variables have higher reliability in the prediction of fatigue parameters.

4. The phase angle, temperature, viscosity and softening point variables have a significant effect on the model output variance.

5. The limitation of the proposed model is the need for large and more comprehensive database to adjust its predictive accuracy.

References

1. Abu El-Maaty Behiry, A.E. Fatigue and rutting lives in flexible pavement. *Ain Shams Eng. J.* **2012**, *3*, 367–374. [CrossRef]

2. Khan, S.; Nagabhushana, M.; Tiwari, D.; Jain, P. Rutting in Flexible Pavement: An Approach of Evaluation with Accelerated Pavement Testing Facility. *Procedia Soc. Behav. Sci.* **2013**, *104*, 149–157. [CrossRef]

3. Mirzababaei, P.; Nejad, F.M.; Vanaei, V. Investigation of rutting performance of asphalt binders containing warm additive. *Pet. Sci. Technol.* **2016**, *35*, 79–85. [CrossRef]

4. Kim, H.; Wagoner, M.P.; Buttlar, W.G. Micromechanical fracture modeling of asphalt concrete using a single-edge notched beam test. *Mater. Struct.* **2008**, *42*, 677–689. [CrossRef]

5. Sani, A.; Hasan, M.R.M.; Shariff, K.A.; Jamshidi, A.; Ibrahim, A.H.; Poovaneshvaran, S. Engineering and microscopic characteristics of natural rubber latex modified binders incorporating silane additive. *Int. J. Pavement Eng.* **2019**, 1–10. [CrossRef]

6. Rahman, M.; Gassman, S.L. Effect of resilient modulus of undisturbed subgrade soils on pavement rutting. *Int. J. Geotech. Eng.* **2017**, *13*, 152–161. [CrossRef]

7. Brown, E.R.; Kandhal, P.S.; Roberts, F.L.; Kim, Y.R.; Lee, D.-Y.; Kennedy, T.W. *Hot Mix Asphalt Materials, Mixture Design and Construction*, 3rd ed.; NAPA Research and Education Foundation: Lanhamm, MD, USA, 2009.

8. Polacco, G.; Filippi, S.; Merusi, F.; Stastna, G. A review of the fundamentals of polymer-modified asphalts: Asphalt/polymer interactions and principles of compatibility. *Adv. Colloid Interface Sci.* **2015**, *224*, 72–112. [CrossRef]

9. Porto, M.; Caputo, P.; Loise, V.; Eskandarsefat, S.; Teltayev, B.; Rossi, C.O. Bitumen and Bitumen Modification: A Review on Latest Advances. *Appl. Sci.* **2019**, *9*, 742. [CrossRef]

10. Alas, M.; Ali, S.I.A. Prediction of the High-Temperature Performance of a Geopolymer Modified Asphalt Binder using Artificial Neural Networks. *Int. J. Technol.* **2019**, *10*, 417. [CrossRef]

11. Kök, B.V.; Yilmaz, M.; Sengoz, B.; Sengur, A.; Avci, E. Investigation of complex modulus of base and SBS modified bitumen with artificial neural networks. *Expert Syst. Appl.* **2010**, *37*, 7775–7780. [CrossRef]

12. Yan, K.; You, L. Investigation of complex modulus of asphalt mastic by artificial neural networks. *Indian J. Eng. Mater. Sci.* **2014**, *21*, 445–450.

13. Cui, L.; Yang, S.; Chen, F.; Ming, Z.; Lu, N.; Qin, J. A survey on application of machine learning for Internet of Things. *Int. J. Mach. Learn. Cybern.* **2018**, *9*, 1399–1417. [CrossRef]

14. Bjornson, E.; Giselsson, P. Two Applications of Deep Learning in the Physical Layer of Communication Systems [Lecture Notes]. *IEEE Signal Process. Mag.* **2020**, *37*, 134–140. [CrossRef]

15. Qin, Z.; Ye, H.; Li, G.Y.; Juang, B.-H.F. Deep Learning in Physical Layer Communications. *IEEE Wirel. Commun.* **2019**, *26*, 93–99. [CrossRef]
16. Voulodimos, A.; Doulamis, N.; Doulamis, A.; Protopapadakis, E. Deep Learning for Computer Vision: A Brief Review. *Comput. Intell. Neurosci.* **2018**, *2018*, 7068349. [CrossRef]
17. Pingel, J.; Ha, G. Deep Learning for Computer Vision. Available online: https://www.mathworks.com/videos/deep-learning-for-computer-vision-120997.html (accessed on 29 June 2019).
18. Li, S.; Zhao, X. Image-Based Concrete Crack Detection Using Convolutional Neural Network and Exhaustive Search Technique. *Adv. Civ. Eng.* **2019**, *2019*, 6520620. [CrossRef]
19. Guo, Y.; Liu, Y.; Oerlemans, A.; Lao, S.; Wu, S.; Lew, M.S. Deep learning for visual understanding: A review. *Neurocomputing* **2016**, *187*, 27–48. [CrossRef]
20. Cao, C.; Liu, F.; Tan, H.; Song, D.; Shu, W.; Li, W.; Zhou, Y.; Bo, X.; Xie, Z. Deep Learning and Its Applications in Biomedicine. *Genom. Proteom. Bioinform.* **2018**, *16*, 17–32. [CrossRef]
21. Lee, T.-L.; Lin, H.-M.; Lu, Y.-P. Assessment of highway slope failure using neural networks. *J. Zhejiang Univ. A* **2009**, *10*, 101–108. [CrossRef]
22. Martinez-Morales, J.; Palacios-Hernández, E.R.; Velázquez-Carrillo, G.A. Modeling and multi-objective optimization of a gasoline engine using neural networks and evolutionary algorithms. *J. Zhejiang Univ. A* **2013**, *14*, 657–670. [CrossRef]
23. Akpinar, P.; Khashman, A. Intelligent classification system for concrete compressive strength. *Procedia Comput. Sci.* **2017**, *120*, 712–718. [CrossRef]
24. Khashman, A.; Akpinar, P. Non-Destructive Prediction of Concrete Compressive Strength Using Neural Networks. *Procedia Comput. Sci.* **2017**, *108*, 2358–2362. [CrossRef]
25. Xi-Zhao, W.; Qing-Yan, S.; Qing, M.; Jun-Hai, Z. Architecture selection for networks trained with extreme learning machine using localized generalization error model. *Neurocomputing* **2013**, *102*, 3–9. [CrossRef]
26. Berka, P.; Rauch, J.; Zighed, D.A. *Data Mining and Medical Knowledge Management: Cases and Applications*; IGI Global: Hershey, PA, USA, 2009; ISBN 9781605662183.
27. Asante-Okyere, S.; Shen, C.; Ziggah, Y.Y.; Rulegeya, M.M.; Zhu, X. Investigating the Predictive Performance of Gaussian Process Regression in Evaluating Reservoir Porosity and Permeability. *Energies* **2018**, *11*, 3261. [CrossRef]
28. Caywood, M.S.; Roberts, D.M.; Colombe, J.B.; Greenwald, H.S.; Weiland, M.Z. Gaussian Process Regression for Predictive But Interpretable Machine Learning Models: An Example of Predicting Mental Workload across Tasks. *Front. Hum. Neurosci.* **2017**, *10*, 647. [CrossRef]
29. Richardson, R.R.; Osborne, M.A.; Howey, D. Gaussian process regression for forecasting battery state of health. *J. Power Sources* **2017**, *357*, 209–219. [CrossRef]
30. Aye, S.; Heyns, P. An integrated Gaussian process regression for prediction of remaining useful life of slow speed bearings based on acoustic emission. *Mech. Syst. Signal Process.* **2017**, *84*, 485–498. [CrossRef]
31. Yu, H.; Wang, Z.; Rezaee, R.; Zhang, Y.; Xiao, L.; Luo, X.; Wang, X.; Zhang, L. The Gaussian Process Regression for TOC Estimation Using Wireline Logs in Shale Gas Reservoirs. In Proceedings of the International Petroleum Technology Conference, Society of Petroleum Engineers (SPE), Bangkok, Thailand, 14–16 November 2016.
32. Fyfe, C.; Der Wang, T.; Chuang, S.J. Comparing Gaussian Processes and Artificial Neural Networks for Forecasting. In Proceedings of the 9th Joint Conference on Information Sciences (JCIS), Kaohsiung, Taiwan, 8–11 October 2006; Atlantis Press: Amsterdam, The Netherlands, 2006; Volume 2006, pp. 29–32.
33. Chaurasia, P.; Younis, K.; Qadri, O.S.; Srivastava, G.; Osama, K. Comparison of Gaussian process regression, artificial neural network, and response surface methodology modeling approaches for predicting drying time of mosambi (Citrus limetta) peel. *J. Food Process. Eng.* **2018**, *42*, e12966. [CrossRef]
34. Ghasemi, P.; Aslani, M.; Rollins, S.D.K.; Williams, R.C. Principal Component Neural Networks for Modeling, Prediction, and Optimization of Hot Mix Asphalt Dynamics Modulus. *Infrastructures* **2019**, *4*, 53. [CrossRef]
35. El-Badawy, S.M.; El-Hakim, R.T.A.; Awed, A. Comparing Artificial Neural Networks with Regression Models for Hot-Mix Asphalt Dynamic Modulus Prediction. *J. Mater. Civ. Eng.* **2018**, *30*, 04018128. [CrossRef]
36. Liu, J.; Yan, K.; Liu, J.; Zhao, X. Using Artificial Neural Networks to Predict the Dynamic Modulus of Asphalt Mixtures Containing Recycled Asphalt Shingles. *J. Mater. Civ. Eng.* **2018**, *30*, 04018051. [CrossRef]
37. De Souza, V.M.A. Asphalt pavement classification using smartphone accelerometer and Complexity Invariant Distance. *Eng. Appl. Artif. Intell.* **2018**, *74*, 198–211. [CrossRef]

38. Chen, C.-L.; Tai, C.-L. Adaptive fuzzy color segmentation with neural network for road detections. *Eng. Appl. Artif. Intell.* **2010**, *23*, 400–410. [CrossRef]

39. Daneshvar, D.; Behnood, A. Estimation of the dynamic modulus of asphalt concretes using random forests algorithm. *Int. J. Pavement Eng.* **2020**, 1–11. [CrossRef]

40. Yu, J. *Modification of Dynamic Modulus Predictive Models for Asphalt Mixtures Containing Recycled Asphalt Shingles*; Iowa State University: Ames, IA, USA, 2018.

41. Bari, J.; Witczak, M.W. Development of a new revised version of the Witczak E Predictive Model for hot mix asphalt mixtures. *Electron. J. Asph. Paving Technol.* **2006**, *75*, 381–423.

42. Akpinar, P.; Uwanuakwa, I.D. Intelligent prediction of concrete carbonation depth using neural networks. *Bull. Transilv. Univ. Braşov. Ser. III Math. Phys.* **2016**, *9*, 99–108.

43. Akpınar, P.; Uwanuakwa, I.D. Investigation of the parameters influencing progress of concrete carbonation depth by using artificial neural networks. *Mater. Constr.* **2020**, *70*, 209. [CrossRef]

44. Wu, C.; Chau, K. Prediction of rainfall time series using modular soft computingmethods. *Eng. Appl. Artif. Intell.* **2013**, *26*, 997–1007. [CrossRef]

45. Al, R.; Behera, C.R.; Zubov, A.; Gernaey, K.V.; Sin, G. Meta-modeling based efficient global sensitivity analysis for wastewater treatment plants—An application to the BSM2 model. *Comput. Chem. Eng.* **2019**, *127*, 233–246. [CrossRef]

46. Liu, X.; Ren, Y.; Song, X.; Witarto, W. A global sensitivity analysis method based on the Gauss-Lobatto integration and its application in layered periodic foundations with initial stress. *Compos. Struct.* **2020**, *244*, 112297. [CrossRef]

47. Zhang, X.-Y.; Trame, M.N.; Lesko, L.J.; Schmidt, S. Sobol Sensitivity Analysis: A Tool to Guide the Development and Evaluation of Systems Pharmacology Models. *CPT Pharmacomet. Syst. Pharmacol.* **2015**, *4*, 69–79. [CrossRef] [PubMed]

48. Saltelli, A.; Ratto, M.; Andres, T.; Campolongo, F.; Cariboni, J.; Gatelli, D.; Saisana, M.; Tarantola, S. *Global Sensitivity Analysis: The Primer*; John Wiley and Sons: Chichester, UK, 2008; ISBN 9780470059975.